Final Technical Report
for
USGS/NEHRP Award Number G15AP00037

Title: Ultrasonic investigations of the micro-mechanical origin of rate and state friction

PI: Allan Rubin
Department of Geosciences
Princeton University, Princeton, N.J. 08544
Phone: (609) 258-1506
Fax: (609) 258-1274
e-mail: arubin@princeton.edu

Award Period: 02/01/2015 – 01/31/2016

Bibliography of publications resulting from this work:

Bhattacharya, P., A.M. Rubin, E. Bayart, H.M. Savage, and C. Marone, 2015, Critical evaluation of state evolution laws in rate and state friction: Fitting large velocity steps in simulated fault gouge with time-, slip- and stress-dependent constitutive laws, *J. Geophys. Res. Solid Earth, 120*, doi:10.1002/2015JB012437.

Bhattacharya, P., A.M. Rubin, and N.M. Beeler, 2017, Does fault strengthening in laboratory rock friction experiments really depend primarily upon time and not slip?, *J. Geophys. Res. Solid Earth, 122*, doi:10.1002/2017JB013936.

1 Abstract

Earthquakes are the culmination of a friction-controlled slip instability on natural faults. The weakening of the interface during the phase of accelerating slip, termed earthquake nucleation, is determined by the frictional properties of the sliding surface. In the absence of in situ constraints on the physics of friction on natural faults, laboratory experiments have guided the design of relevant constitutive equations. Rate and state friction is the most widely used representative of this class of friction theories.

The formulation of rate and state friction requires an equation for the time evolution of 'state', a proxy for the real area and quality of contacts bridging the frictional interface. However, the most widely used Aging and Slip state evolution laws are both deficient in their ability to explain the full range of laboratory experiments. It has long been claimed that the slip-dependent evolution of the Slip law better models velocity step experiments, while the time-dependent evolution of the Aging law better models slide-hold-slide experiments. To the extent that large velocity decreases and holds access similar parts of parameter space, this accepted view is not internally consistent. We re-analyze the slide-hold-slide experiments of Beeler et al. [1994], long considered to have established that healing during the holds is time-dependent (Aging law) rather than slip dependent (Slip law). We show analytically and by Bayesian inversion that in fact the continual and stiffness-dependent stress relaxation during the holds is modeled very well by the Slip law, but is incompatible with the Aging law with constant rate-state parameters. Additionally, although neither law provides a good fit to both the stress relaxation during the holds and the stress peaks following the resides, the Slip-law fit is superior.

Given the evidence for the increase in contact area with time during stationary holds, but the apparent lack of time-dependent strengthening during the holds in slide-hold-slide experiments, we used ultrasonic monitoring of the sliding interface to provide additional information concerning fault 'state'. We carried out velocity step increases and decreases of 1–3 orders of magnitude, and slide-hold-reslide experiments with holds of up to 5000s duration, at slip speeds of 3–100 μm/s. The interface was probed with ultrasonic shear waves of frequency 0.5 MHz at 1000 shots per second, recorded at 25 MHz. Mode conversion of S- to P-waves allowed us to measure changes in both P- and S-wave transmissivity and travel time during the experiments. As expected, we find systematic increases in transmissivity and decreases in travel time with decreases in slip speed from steady state, and vice-versa for increases in slip speed. For purely elastic contacts across the interface, percentage changes in P- and S-wave transmissivity are expected to be proportional. That we see larger percentage changes in S-wave than in P-wave transmissivity is indicative of inelastic deformation at these contacts at ultrasonic frequencies, and seems qualitatively consistent with differential slip at the margins of contacts produced by wave-induced changes in shear stress.

2 Introduction

For a fault to fail repeatedly during successive seismic cycles, it is necessary for it to strengthen (heal) during the interseismic period. Friction experiments on both bare rock and gouge have shown

that the slip interface strengthens during periods of little or no sliding called holds [Dieterich, 1972, Beeler et al., 1994, Dieterich and Kilgore, 1994, Nakatani and Mochizuki, 1996, Marone, 1998, Berthoud et al., 1999, Bureau et al., 2002, Marone and Saffer, 2015]. This strengthening is evidenced by the fact that the peak static friction upon resliding is an increasing function of the duration of the preceding hold [Beeler et al., 1994, Marone, 1998, Berthoud et al., 1999]. On initially bare rock surfaces, such frictional strengthening has two robust characteristics: (1) The static friction peaks increase linearly with the logarithm of the hold time for holds longer than a threshold time of order seconds [Dieterich, 1972, Beeler et al., 1994, Marone, 1998, Berthoud et al., 1999]; (2) This constant rate of healing/strengthening is independent of the stiffness of the testing apparatus [Beeler et al., 1994] (by 'rate of healing/strengthening' we mean the rate of increase in static friction with log hold time, as evidenced by the peak stress following a reslide).

Observation (1) is not limited to bare rock surfaces; such log linear healing with hold time has been reported for a wide range of materials, e.g., simulated gouge [Karner and Marone, 1998, 2001], steel [Dokos, 1946], PMMA [Berthoud et al., 1999], and paper [Heslot et al., 1994]. It is noteworthy that the rates of healing across these materials are remarkably similar, $\sim 10^{-2}$ per decade of hold duration. This points to a robust and (perhaps) material-independent physical or chemical mechanism governing frictional healing [Berthoud et al., 1999, Bureau et al., 2002]. Since different stiffnesses lead to different amounts of slip during the holds, observation (2) was used by Beeler et al. [1994]] to infer that this mechanism is dominantly time dependent, i.e., frictional interfaces heal even at rest as the logarithm of the hold time. Such an inference is consistent with observations of time-dependent growth of the size of microcontacts bridging stationary interfaces, as revealed by direct optical measurements in Lucite acrylic and soda glass [Dieterich and Kilgore, 1994]. Furthermore, observations of continued increase in static friction peaks with hold duration even at near-zero shear stresses (thus ensuring near-zero slip) for a variety of materials, including granite, also lends support to the suggestion that slip might not be necessary for frictional healing [Nakatani and Mochizuki, 1996, Bureau et al., 2002]. All of these lines of evidence seem to suggest that time-dependent healing is a desirable property in constitutive relations of fault friction.

The most widely used constitutive relations for fault friction are the laboratory-derived rate-and-state friction (RSF) equations. Robust laboratory observations have established the dependence of friction on slip rate and 'state' (some measure of the quality and/or quantity of true contact area). But a single mathematical description of the evolution of the state variable that agrees with the full range of laboratory friction data remains elusive. This is due at least in part to the inherent problems in directly monitoring the contact-scale mechanics of slip interfaces in rocks which, in turn, has resulted in the lack of experimental constraints to help guide our theoretical understanding of 'state'. Within the RSF framework there are two end-member views of how frictional state evolves: (a) the Slip law [Ruina, 1983], which allows state to evolve only with slip, and (b) the Aging law [Dieterich, 1978, Ruina, 1983], which allows state to evolve even without slip, purely as a function of time. Beeler et al. [1994] used observation (2) above, and numerical simulations, to conclude that their data supported Aging law style time-dependent healing. Since typical laboratory holds subject the interface to rates of sliding many orders of magnitude smaller than the steady state sliding speed prior to the hold, a corollary of this conclusion is that the Aging law is the appropriate friction constitutive description at such small slip rates.

However, it has long been recognized that velocity-step experiments are consistently better ex-

plained by the Slip law than by the Aging law. Bhattacharya and Rubin [2014] and Bhattacharya et al. [2015] recently extended these results to sequences of 2–3-order velocity step increases and decreases on simulated gouge, which rapidly imposed slip rates orders of magnitude larger or smaller than the preceding steady state rate on the sliding interface. Given that large velocity step decreases also access sliding regimes which promote frictional healing (brought about by the rapid deceleration from steady state sliding), it seems inconsistent to simultaneously claim that (1) fault healing in rock is primarily time dependent and (2) large velocity decreases are well modeled by the Slip law and not the Aging law.

As part of this work we investigated this inconsistency by reanalyzing the data of Beeler et al. [1994]. We focused not only on the static friction peaks but also on the stress relaxation during the holds. We carried out detailed nonlinear inversions on the initially bare rock data from Beeler et al. [1994] to examine the Aging and Slip law fits to the stress relaxation during holds both in isolation and in conjunction with the evolution of static friction peaks with hold time. Additionally, we used two other laws – a Slip/Aging hybrid evolution law, and a recently proposed shear stress-dependent evolution law – both of which can be tuned to transition between Aging and Slip law behaviors to check if the data are better explained by a (particular) combination of Aging and Slip rather than Aging or Slip alone. We compared the properties of these fits with analytical predictions of the frictional response to long holds under the different formulations of RSF considered here.

Our results reveal that stiffness independence of the healing rate is not sufficient to rule out the Slip law; in fact, it is possible to find Slip law parameters that fit the peak stress data as well as the Aging law does. Additionally, we point out that, vis-a-vis the Aging versus Slip argument, the more diagnostic (and robust) feature of the Beeler et al. [1994] data is the strongly stiffness dependent rate of stress relaxation during holds, provided we consider the RSF parameters to be constant. Using both analytical and inversion results, we show that such data are consistent with the Slip law and, importantly, are sufficient to rule out the Aging law with constant RSF parameters. To relax this constraint, some of our inversions also introduced velocity-dependent RSF parameters designed to add stiffness sensitivity to the otherwise stiffness-independent rates of stress relaxation under the Aging law [Bhattacharya et al., 2017]. But the specific formulations of velocity dependence chosen in that study seem to not help the Aging law improve its fits to the holds. Finally, when fitting both peak stresses and the stress minima at the end of holds together, all our inversions, including the ones with nonconstant RSF parameters, show that the Slip law fits the slide-hold-slide data consistently better than the Aging law. We also ran all of these inversions with two alternative state evolution prescriptions – a stress-dependent law and an Aging-Slip hybrid – both of which replicated the respective best Slip law fits despite the freedom of an additional tunable parameter.

3 Rate-and-state background

RSF describes the frictional strength of an interface as a function of two variables: the sliding rate, V, and the state, θ, a proxy (in units of time for the state evolution formulations we have chosen) for the strength of the asperities in contact across the sliding interface at a reference slip speed, often considered to scale with the true area of contact [Linker and Dieterich, 1992, Baumberger and Caroli, 2006]. These variables are related by two coupled equations. The first of these, called

the friction law, describes the rate and state dependence of frictional strength:

$$\frac{\tau}{\sigma} = \mu(V,\theta) = \mu_* + a \ln \frac{V}{V_*} + b \ln \frac{\theta}{\theta_*} \ , \tag{1}$$

where τ is frictional strength, σ is normal stress, μ is the "rate-and-state-dependent" friction coefficient, a is the "direct effect" parameter accounting for the variations in frictional strength due to changes in slip rate, and b is the "evolution effect" parameter which determines the change in friction due to evolution of state. In general, at not very high temperatures, a and b are constants of the order of 0.01, but they can vary by as much as an order of magnitude with varying temperature and moisture content [Blanpied et al., 1998]. The other parameters μ_*, V_*, and θ_* are the values of friction coefficient, slip rate, and state at an arbitrary reference steady state. The system of equations is closed with an evolution equation for θ. The two most widely used forms are

$$\text{Aging (Dieterich) law: } \dot{\theta} = 1 - \frac{V\theta}{D_c} \tag{2}$$

$$\text{Slip (Ruina) law: } \dot{\theta} = -\frac{V\theta}{D_c} \ln \frac{V\theta}{D_c} \tag{3}$$

where the overdot denotes the time derivative and D_c is a characteristic slip scale for state evolution [Dieterich, 1978, Ruina, 1983]. Equation (2) is often referred to as the Aging law, because state increases linearly with time for stationary contacts. Equation (3) is referred to as the Slip law, as state evolution occurs only for slipping contacts ($\lim_{(V\to 0)} \dot{\theta} = 0$). At steady state sliding ($\dot{\theta} = 0$), both laws yield $V\theta/D_c = 1$. We refer to $V\theta/D_c > 1$ and $V\theta/D_c < 1$ as being "above" and "below" steady state, respectively; we use the phrase "far from steady state" to imply $V\theta/D_c$ significantly different from 1.

Given that at steady state $V\theta/D_c = 1$, equation (1) leads to the following expression for the change in frictional strength between two steady states at velocities V_2 and V_1:

$$\frac{\Delta\tau}{\sigma} = (a-b) \ln \frac{V_2}{V_1} \ . \tag{4}$$

For $(a-b) < 0$ the sliding surface is steady-state velocity weakening and can undergo velocity instabilities when the sliding is perturbed from steady state. For $(a-b) > 0$ (steady-state velocity strengthening) such instabilities are not possible.

3.1 Implications of Velocity Step Tests

One robust observation from large velocity steps (of $\sim 1-3$ orders of magnitude) on both initially bare rock surfaces and synthetic gouge is that the evolution of frictional strength following the rapid extremum occurs over a quasi-constant slip scale, independent of the magnitude or sign of the step [Ruina, 1980, 1983, Tullis and Weeks, 1986, Bhattacharya et al., 2015]. Consistent with such data, the Slip law predicts an exponential approach to steady state over a characteristic slip scale D_c following a velocity step of arbitrary size or sign [Rice, 1993, Nakatani, 2001, Ampuero and Rubin, 2008].

In contrast, the evolution of frictional strength under the Aging law following a large velocity step occurs over slip scales which are functions of both the magnitude and sign of the step. Such asymmetry is fundamentally tied to the relative amplitude of the two terms on the right side of equation (2). For a large and sudden velocity increase, the surface is far above steady state ($V\theta/D_c \gg 1$) and one can neglect the "1" in equation (2). Integrating the resulting equations under the assumption of constant slip speed and plugging the result into (1) leads to linear slip weakening with slope $b\sigma/D_c$. That the rate of slip weakening is independent of the size of the velocity step implies that the evolution of frictional strength to steady state occurs over length scales which increase with the size of the jump [Ruina, 1980, Nakatani, 2001, Rubin and Ampuero, 2005]. On the other hand, for a velocity step decrease large and rapid enough to instantaneously satisfy $V\theta/D_c \ll 1$, Aging law state evolution predicts $\dot{\theta} \sim 1$; i.e., there is no slip scale for state evolution. In this limit, the post-step increase in state is just time elapsed since the velocity step, and significant state evolution occurs over slip distances $\delta \ll D_c$ [Ampuero and Rubin, 2008]. As mentioned above, such asymmetry in the frictional response between large velocity increases and decreases is not supported by observations from velocity step experiments.

Large velocity step decreases and long holds are intimately connected in that they both access the portion of the parameter space where $V\theta/D_c \ll 1$, even though the slip rates at the end of long holds are much lower. Therefore, it seems inconsistent that one of these types of experiments would provide evidence for dominantly slip-dependent healing while the other for time dependence. It is then reasonable to ask if the Aging law is capable of providing a reasonable fit to large velocity decrease data alone. For ideal velocity step decreases, the expectation is that the Aging law slip-strengthening length scale should decrease with increasing step size, while for the Slip law, one would expect slip to evolve over the same characteristic length scale for all step sizes (Figure 1a). Bhattacharya et al. [2015] reported some near-ideal 1–2-order velocity steps on simulated gouge (data set p1060 therein), which clearly show that friction evolves over a constant length scale following these large step decreases in slip rate, consistent with the Slip law (Figure 1b). In fact, the Aging law clearly performs worse than the Slip law when constrained to fit the 1- and 2-order step decreases alone (Figure 1c). It is also noteworthy that the Slip law parameters adopted to fit the step decreases also fit the step increases very well. Therefore, the Aging law, and its prediction that $\dot{\theta} \sim 1$ when $V\theta/D_c \ll 1$, are not supported by laboratory velocity step data which access sliding regimes far below steady state. It is also important to recognize that the Aging law's apparent success in explaining the peak stress upon reslides following laboratory holds originates from the very ingredient that leads to its failure in fitting the velocity step decrease data: time-dependent healing [Bhattacharya et al., 2017]. These observations provided the motivation for our reexamination of the slide-hold-slide data set of Beeler et al. [1994].

3.2 Implications of Slide-Hold-Slide Tests

In a typical slide-hold-slide (SHS) test, the shear stress on an interface undergoing steady sliding at a rate $V_{s/r}$ is relaxed by bringing the load point abruptly to rest. After being held for some duration t_{hold}, the load point is redriven at the prehold speed. This increases the stress until the slider is slipping as fast as the load point. Beyond this peak friction, stress decays back to steady state with continued sliding. The difference between peak stress and the future steady state ($\Delta\mu_{peak}$) has traditionally been used as a measure of frictional healing/strengthening during the preceding

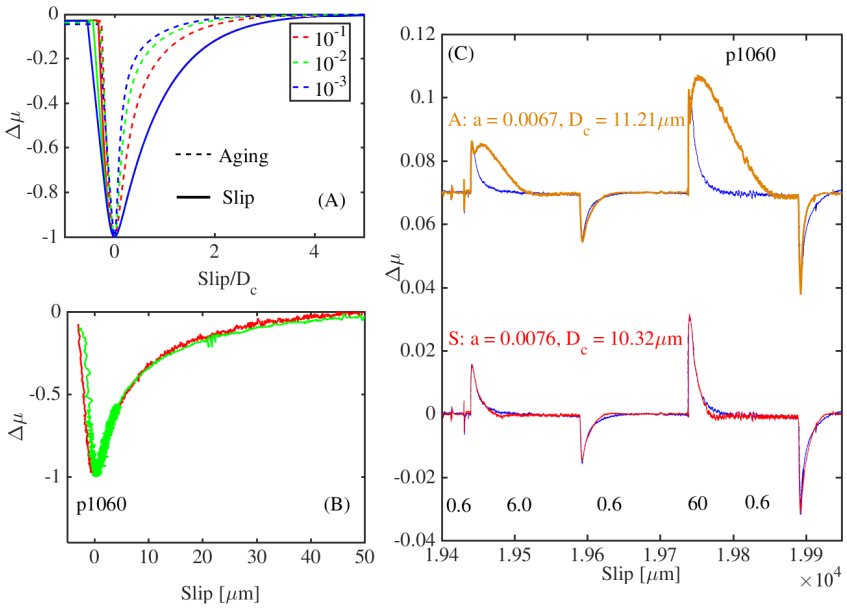

Figure 1: (a) Numerical solution of the response of Aging (dashed lines) and Slip (solid lines) laws to velocity step decreases of 1 (red), 2 (green), and 3 (blue) orders of magnitude. The simulations use the best fitting Slip law parameters from Figure 1c and the appropriate stiffness 0.008 μm/s. Friction values are normalized by minimum-to-residual stress change. Following the stress minimum, the Slip law curves for the different orders of magnitude plot on the top of each other. (b) Change in friction as a function of slip for load point velocity decreases of 1 and 2 orders of magnitude in simulated gouge [Bhattacharya et al., 2015]. The data are scaled to the minimum-to-residual friction range as in Figure 1a. These large velocity steps carry the surface far below steady state, yet the data for the 1 and 2 order of magnitude steps strengthen over the same slip distance, as predicted by the Slip law in Figure 1a. (c) Aging and Slip law fits to the velocity step data shown in Figure 1b. Only the velocity step decreases were fit with the 1- and 2-order decreases equally weighted. We constrained $a - b = -0.0002$. Blue, Data; Ochre, Aging law; Red, Slip law. Numbers in black denote load point displacement rate in μm/s.

hold (Figure 2).

Beeler et al. [1994] studied the evolution of $\Delta\mu_{peak}$ with t_{hold} in initially bare granite and quartzite by carrying out a sequence of SHS tests with holds from $\sim 10^{-0.5} - 10^{4.5}$s. This sequence of holds was repeated under two different setups of the testing apparatus which resulted in effective stiffnesses that differed by a factor of 30. Their data show that $\Delta\mu_{peak}$ increases as a linear function of the logarithm of hold time such that the slope (i.e. the healing rate) is independent of stiffness (Figure 2c). Beeler et al. [1994] argued, based on this observation and numerical simulations, that the stiffness independence of the evolution of $\Delta\mu_{peak}$ supported continued strengthening of nearly stationary interfaces with time as formulated by the Aging law. They further argued that the Slip law predicts stiffness-dependent healing rates, since the amount of slip accrued during the hold, and hence the concomitant state evolution, is stiffness dependent. We showed that some of these conclusions are suspect, and that furthermore there are other properties of the data which provide more reliable diagnostic constraints on the class of state evolution laws that we are considering, provided a, b, and D_c are constants across the range of velocities accessed in the experiment.

It is first worth noting that the main purpose of these experiments was to determine the amount of

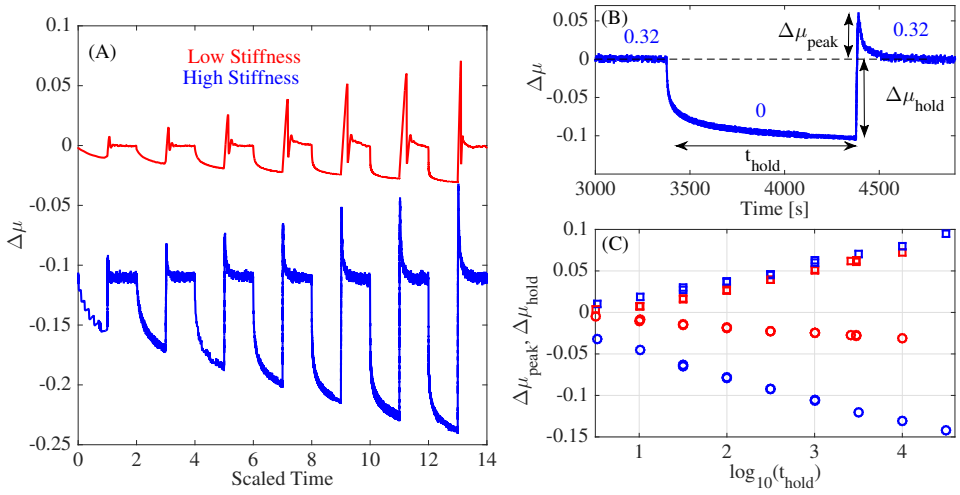

Figure 2: (a) Shear stress evolution from the slide-hold-slides of Beeler et al. [1994]. The X axis is time, scaled such that each phase of hold and slide/reslide has unit duration to aid in visualization. The holds span $10^{0.5} - 10^4$ s in t_{hold}. The red curve shows a slide-hold-slide sequence for the lower, natural stiffness setup ($k_n = 0.0019\mu$/m, $V_{s/r} = 1.0\mu$m/s), the blue curve shows a sequence for the stiffer apparatus ($k_s = 0.055\mu$/m, $V_{s/r} = 0.32\mu$m/s). (b) A 1000 s hold with the stiffer apparatus. The t_{hold}, $\Delta\mu_{peak}$, and $\Delta\mu_{hold}$ notation wherever used in the text is as defined in this figure. Numbers in blue represent load point velocities in μm/s. (c) Evolution of $\Delta\mu_{peak}$ (squares) and $\Delta\mu_{hold}$ (circles) with t_{hold} for two sets of slide-hold-slide sequences with the low (red) and high (blue) stiffness setups. The time evolution of these quantities is remarkably reproducible from repeated experiments during the same experimental run.

frictional healing (increase in state) during the holds. The peak stress upon reslide was used as a proxy for this healing only because there is no way to estimate 'state' at the end of the hold directly. However, using peak stress for this purpose requires either negligible reduction of state between the start of the reside and peak stress (when the slip speed equals the load point velocity), or at least that (the logarithm of) this state reduction is independent of hold time, such that the slope of the healing curve reflects the state increase during the hold. Regarding the latter possibility, Beeler et al. [1994] claimed, and we proved under fairly non-restrictive conditions [Bhattacharya et al., 2017], that for the Aging law the change in log(state) between the start of the reside and peak stress is indeed independent of hold duration. However, Bhattacharya et al. [2017] further showed that this property of the Aging law derives entirely from its prediction that well above steady state the fault weakens linearly with slip, at a rate that is independent of $V\theta/D_c$, a prediction that is violated by all relevant experimental data. As a corollary, they showed numerically that for the Slip law, there exists combinations of model parameters such that the stiffness-dependence of the state increase during the hold is largely offset by the stiffness-dependence of the loss in state across the reside, such that for a limited range of parameters the Slip law can fit the Beeler et al. [1994] peak stress data as well as the Aging law can. Finally, that state might be reduced considerably between the start of the reside and peak stress was suggested by the lucite experiments of Dieterich and Kilgore [1994], who showed (their Figure 7) that there was significantly more loss of contact area (transmitted light) between the end of the hold and the attainment of peak stress than would be predicted by state evolution under the Aging or Slip laws. The stressing-rate dependence of the Nagata law is one such mechanism by which this could occur.

For all these reasons we chose to model the stress relaxation during the hold as well as the peak

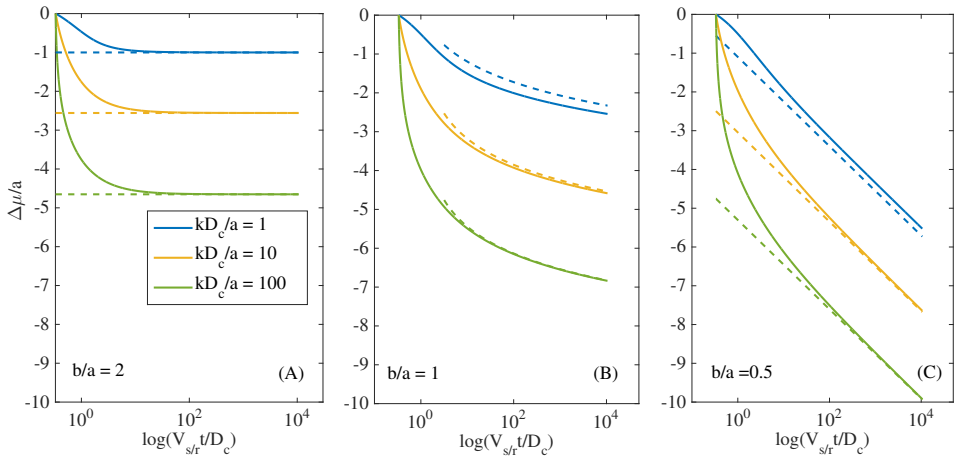

Figure 3: Evolution of frictional strength under the Aging law during a long hold ($\sim 3 \times 10^4$ s) for different values of normalized stiffness, $kD_c/a = 1$ (blue), 10 (ochre), and 100 (green), and different values of b/a. (a) Velocity weakening, $b/a = 2$; (b) Velocity neutral, $b/a = 1$; (c) Velocity strengthening, $b/a = 0.5$. The solid lines show numerical solutions, corresponding dashed lines denote the analytical approximations to $\Delta\mu/a$ derived in section C1 of Bhattacharya et al. [2017]. A velocity-weakening Aging law predicts a constant stress solution for long holds. Velocity-neutral and velocity-strengthening solutions show continual relaxation of stress, but importantly, the rate of stress relaxation for long holds is stiffness independent. Note that the experiments of Beeler et al. [1994] span the range from 0.3 to 1.0 $\lesssim V_{s/r} t_{hold}/D_c \lesssim 3 \times 10^3$ to 10^4 between the high and normal stiffness holds respectively.

stress upon reslide when re-examining the Beeler et al. data. One of the most robust features of these data is the continual decay of stress with log hold time, at a rate that is much larger for the higher-stiffest testing apparatus. In fact, these features are much more consistent with the predictions of the Slip law than the Aging law. From velocity-step tests during the same experimental runs, we know that the granite and quartzite samples of Beeler et al. [1994] were steady-state velocity weakening. For velocity-weakening materials, the Aging law predicts not a continual decay of stress with log hold time, but decay to a constant value that depends upon the stiffness of the testing apparatus (Fig. 3a). The cause is the same as that which gives rise to a healing rate that is independent of stiffness – time-dependent hearing. The sliding surface asymptotically approaches a constant slip distance because the fault is strengthening even as the slip speed approaches zero. For a velocity-strengthening surface the stress continues to decay with hold time (it must, because the surface remains below steady state as the velocity decreases, and the definition of a velocity-strengthening surface is that the steady-state stress decreases as the velocity decreases), but the rate of stress decay with log hold time is independent of the machine stiffness (Fig. 3c). In contrast, the Slip law naturally gives rise to a continual stress decay with log hold time that is greater for the higher stiffness apparatus, because the higher stiffness apparatus produces less slip and less healing of the sliding surface (Fig. 4).

All of these attributes manifest themselves when fitting the data using the Markov Chain Monte Carlo (MCMC) technique of Bhattacharya et al. [2015]. When fitting $\Delta\mu_{peak}$ alone, with $(a - b)$ constrained from velocity steps, the aging law can fit the the healing rate very well (Fig. 5a). However, the stress decay during the holds is both too little (because the surface strengthens too much) and asymptotically approaches a constant value. Relaxing the constraint on $(a - b)$, the

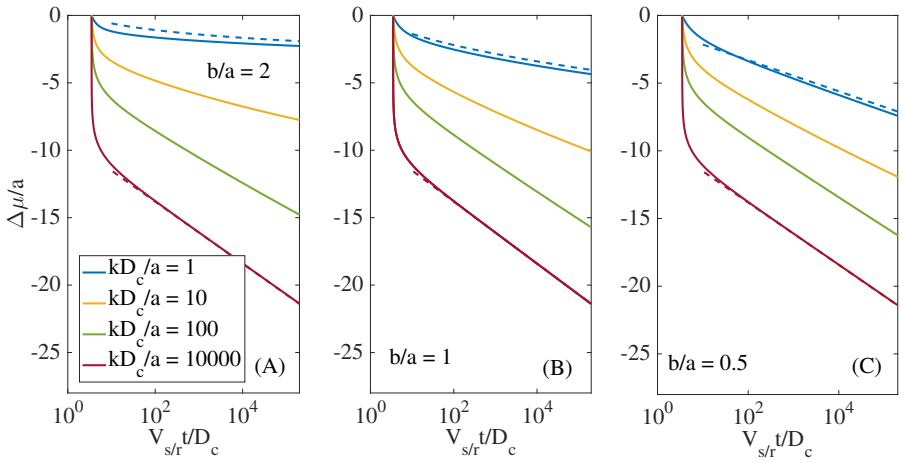

Figure 4: Stress relaxation under the Slip law during a long hold ($\sim 10^5$ s) for different values of the normalized stiffness, $kD_c/a = 1$ (blue), 10 (ochre), and 100 (green), and different values of b/a. (a) Velocity weakening, $b/a = 2$, (b) velocity neutral, $b/a = 1$, and (c) velocity strengthening, $b/a = 0.5$. The solid color lines are the numerically integrated values of $\Delta\mu/a$. Corresponding dashed lines denote the relevant analytical approximations derived in section C2 of Bhattacharya et al. [2017]. In the small stiffness limit (dashed blue lines), the velocity-weakening Slip law predicts a $\log(\log(t_{hold}))$ trajectory, while the velocity strengthening trajectories are linear in $\log(t_{hold})$. The large stiffness limit for all trajectories is $\Delta\mu/a = \ln(V/V_{s/r})$ (dashed red lines).

Aging law can recover the separation of $\Delta\mu_{peak}$ between the high- and low-stiffness apparatus, but still fails to reproduce the observed stress decay during the holds (Fig. 5b). Figure 5b also shows that with $(a-b)$ unconstrained, the Slip law can reproduce the $\Delta\mu_{peak}$ values as well as the Aging law can, although with a value of $(a-b)$ (-0.0001) that is farther from the value determined from the velocity steps (-0.0027) than is the value for the comparable Aging law fit (-0.0007). In addition, the value of D_c adopted by the Slip law fit is farther from the expected value of $1-2\mu$m than is the comparable value for the Aging law. For the Slip law, a small value allows more state evolution between the onset of the reslide and peak stress for the lower stiffness setup, which offsets the greater healing (because of more slip) for that lower stiffness setup.

When fitting the $\Delta\mu_{hold}$ data only (Fig. 6), the Slip law does a better job both with $(a-b)$ constrained (left) and $(a-b)$ unconstrained (right). With $(a-b)$ unconstrained, the Aging law achieves continual stress decay by making the surface velocity strengthening $(a-b=+0.0033)$, but even so the rate of decay for the longest holds is asymptotically the same for the high- and low-stiffness setup, unlike the data but as predicted by our theoretical results. For the unconstrained Slip law, the fit to the $\Delta\mu_{hold}$ data is quite good, and additionally the fit to the $\Delta\mu_{peak}$ data is much better than for the Aging law, with a velocity-weakening surface $(a-b=-0.0003)$ and a reasonable value of D_c.

When fitting both the $\Delta\mu_{peak}$ and the $\Delta\mu_{hold}$ data, with $(a-b)$ constrained both the Aging law and the Slip law fits are poor (Fig. 7). With $(a-b)$ unconstrained, the Slip law fit is superior and is achieved with a value of $(a-b)$ that, although it is velocity strengthening $(a-b=+0.003)$, is less strengthening than for the Aging law fit $(a-b=+0.0047)$. The Aging law fit again has the property that the rate of stress decay during the holds is asymptotically the same for the low- and

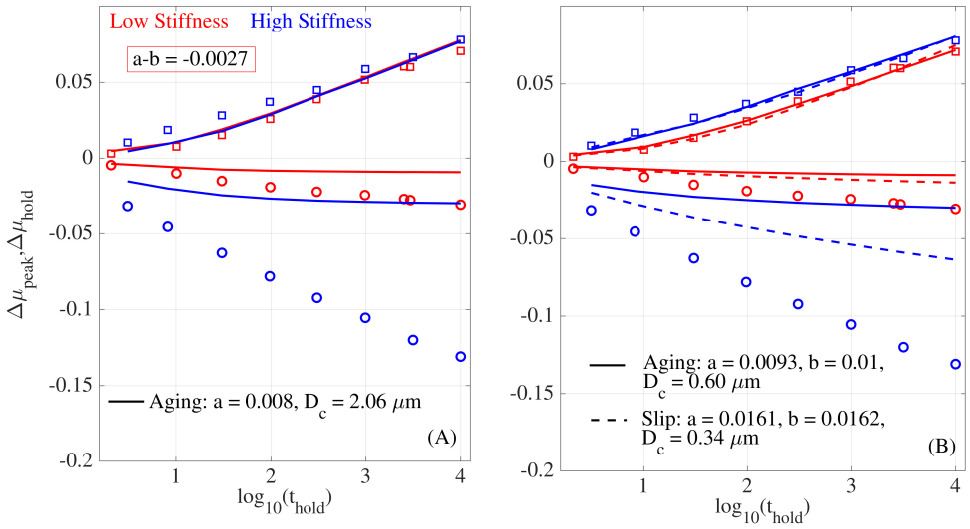

Figure 5: Aging and Slip law fits to the time evolution of $\Delta\mu_{peak}$ in initially bare granite from Beeler et al. [1994]. The red squares and circles are the low stiffness data, the corresponding blue symbols are the high stiffness data. (a) Aging law fit (solid line) with $a-b$ fixed at –0.0027. (b) Aging (solid line) and Slip law (dashed line) fits without any constraint on $a-b$. Note that the Slip law fit to the time evolution of $\Delta\mu_{peak}$ is as good as the Aging law with the healing rate being stiffness independent. However, for both the Aging and Slip laws, the parameter choices that fit the peaks very well completely fail to match the corresponding values of $\Delta\mu_{hold}$.

high-stiffness data.

From our results, we conclude that there is no evidence from the Beeler et al. [1994] data that fault strengthening during long holds is time-dependent rather than slip-dependent. Fitting only the $\Delta\mu_{peak}$ data with the Aging law is problematic (the Aging-law fit relies on a property that is known to be violated by rock friction data), but even so the Slip law can fit the data about as well as the Aging law. Fitting only the $\Delta\mu_{hold}$ data, the Slip law fit is quite good with $(a-b)$ constrained and excellent with $(a-b)$ unconstrained. In the latter case the fitting parameters have the surface velocity-weakening with a reasonable value of D_c, and do a decent job of fitting the $\Delta\mu_{peak}$ data. Fitting all the data, both laws are deficient but the Slip law fit is superior. Finally, given that these conclusions conflict with 2 decades of conventional wisdom regarding these data, we tested two additional state evolution laws proposed by Kato and Tullis [2001] and Nagata et al. [2012]. In each of these cases an additional parameter has been added (in the former case to the Slip law; in the latter case to the Aging law) that allows the laws to toggle between Aging and Slip depending upon the value of that parameter. We found that the MCMC inversions chose values for these additional parameters that made the fits indistinguishable from the best Slip law fit; that is, the inversions preferred the Slip law even given the choice of this additional parameter [Bhattacharya et al., 2017, Figures 11 and 12).

One enduring appeal of Aging law state evolution is that time-dependent healing has a clear, experimentally supported, physical picture in the limit of a truly stationary interface: the growth of contact area with time [Dieterich and Kilgore, 1994], and it's corollaries, normal closure of the sliding interface and increase in acoustic transmissivity [Nagata et al., 2012, Kilgore et al., 2012].

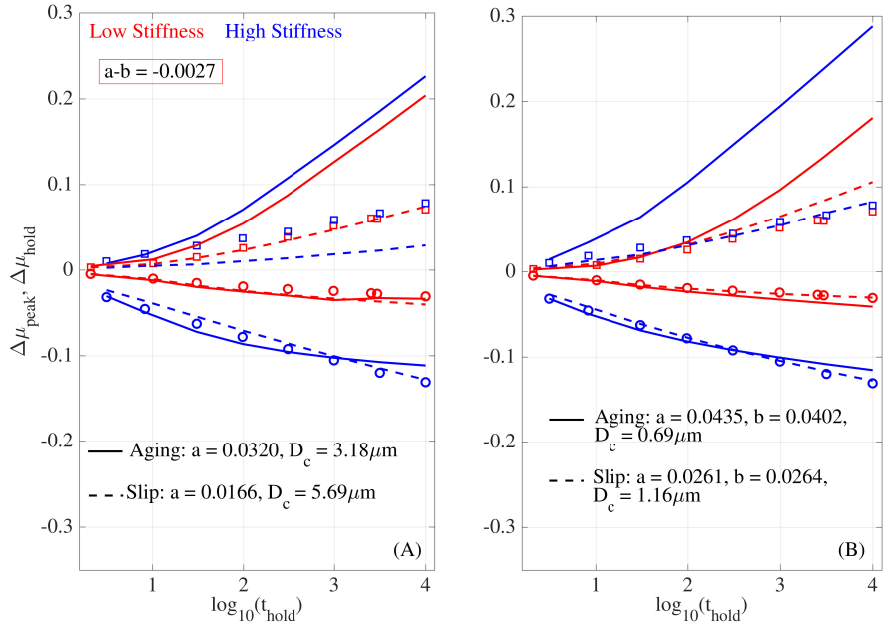

Figure 6: Aging and Slip law fits to the time evolution of $\Delta\mu_{hold}$ in initially bare granite from Beeler et al. [1994]. (a) Aging law (solid line) and Slip law (dashed line) fits with $a-b$ fixed at –0.0027. (b) Fits without any constraint on $a-b$. The Aging law fit is shown with solid lines and the Slip law with dashed lines.

However, the systematic lack of support for the Aging law from long laboratory holds, and its clear refutation by large velocity step decreases, seems an equally compelling argument against Aging law style time-dependent healing when the interface is sliding far below steady state. Our results make it clear that the Aging law cannot explain the friction evolution observed during long laboratory holds with constant RSF parameters. Therefore, one way to reconcile Aging law style time-dependent healing with laboratory hold data is to consider physical mechanisms by which RSF parameters could vary at the low slip rates accessed at the end of long holds. As a first step, we restricted our attention to only those mechanisms which could be modeled through rate dependencies of a and/or b [Boettcher et al., 2007, Rice et al., 2001].

Such an idea is not entirely without experimental motivation. For example, Marone and Saffer [2015] pointed out that $\Delta\mu_{peak}$ and $\Delta\mu_{hold}$ data from simulated gouge show systematic dependencies on $V_{s/r}$ which are not consistent with conventional RSF (with constant parameters) from the point of view of dimensional analysis. One way to explain such systematic loading rate dependence is to add a second velocity scale to traditional RSF models, a particular example of such a modification being rate dependence of a and/or b. We explored two such choices of rate dependence [Bhattacharya et al., 2017], both of which were motivated by the micromechanics of contacting asperities: (1) A strain rate dependence of a (with constant b) derived from the micromechanics of contact creep; (2) An effective rate dependence of $a-b$ brought about by the inclusion of (conventionally neglected) second-order terms in RSF. Both these modifications introduce (1) continual weakening of the interface at progressively smaller slip rates even when the interface is velocity weakening at the reference slip rate $V_{s/r}$, and (2) stiffness-dependent rates of stress relaxation during long holds, both

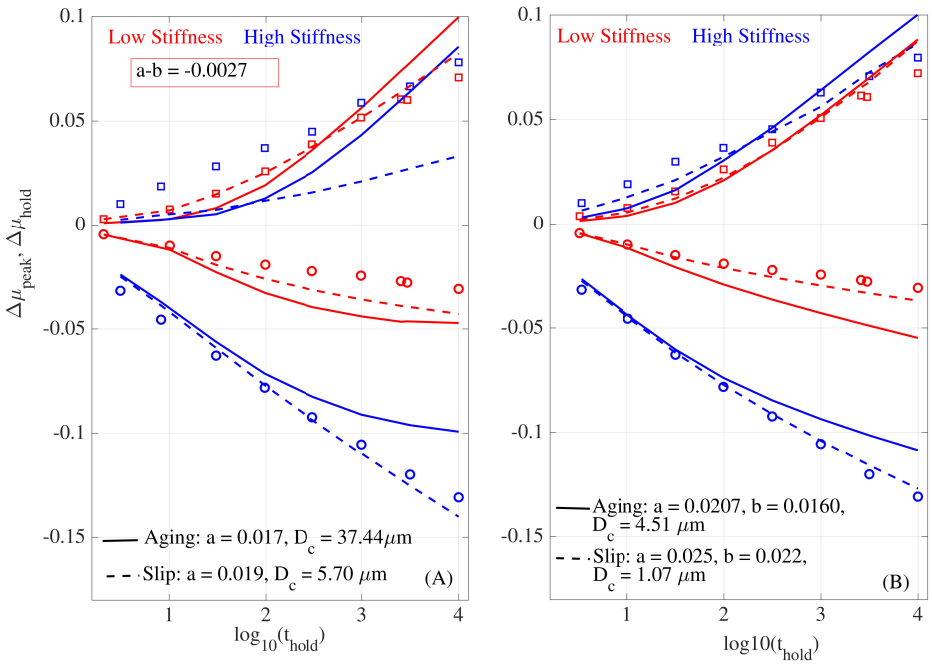

Figure 7: Aging and Slip law fits to the time evolution of both $\Delta\mu_{peak}$ and $\Delta\mu_{hold}$ in initially bare granite from Beeler et al. [1994]. (a) Aging law (solid line) and Slip law (dashed line) fits with $(a-b)$ fixed at –0.0027. (b) Fits without any constraint on $(a-b)$; the solid lines show Aging and the dashed lines Slip law fits.

desirable properties in order for the Aging law to better fit the holds. However, in our inversions, neither of these modifications qualitatively improved the Aging law fits to $\Delta\mu_{peak}$ and $\Delta\mu_{hold}$. Surprisingly, at least one of these formulations (with a increasing logarithmically with decreasing slip rate) actually improved the Slip law fit to the $\Delta\mu_{peak}$ and $\Delta\mu_{hold}$ data. Additionally, this Slip law fit adopted physically reasonable values for the extra parameters introduced due to the rate dependence of a [Bhattacharya et al., 2017, Figure E1]. However, since our choice of these modifications clearly was not exhaustive, this exercise does not rule out the possibility that some other formulation of rate-dependent RSF parameters could address the lack of experimental support for the Aging law.

4 Motivation for using ultrasonic monitoring in rock friction experiments

One of the major impediments to the formulation of a set of rate-state friction constitutive relationships that agree well with the full range of laboratory friction experiments is the lack of direct observational constraints on the contact-scale properties that contribute to 'state'. While there have been previous attempts at optically monitoring the evolution of micro-asperities bridging the frictional interface in transparent plastic [Dieterich and Kilgore, 1994], Nagata et al. [2014] have recently shown that ultrasonic measurements add independent information to our knowledge of

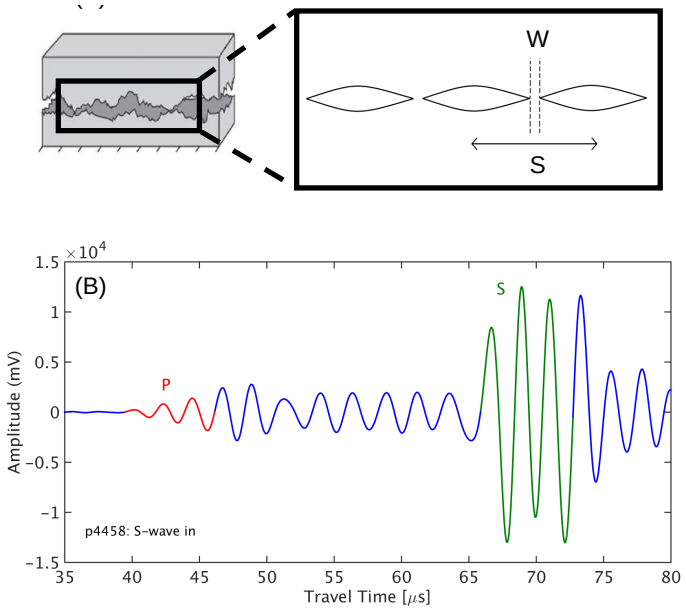

Figure 8: (A): Frictional interface represented as a periodic array of cracks.(B): Typical stacked waveform showing ultrasonic P- (mode converted) and S- transmitted amplitudes in our experiments on bare granite.

the mechanical properties of such an interface. For opaque interfaces like bare granite, ultrasonic monitoring techniques seem especially informative when used to complement mechanical data derived from friction experiments. Our experiments differ from such attempts in the past [Nagata et al., 2008, 2012] in that we simultaneously measure the transmitted (mode converted) P- and S-phases in our experiments to better probe the contact scale rheology. In particular, given the traditional expectation that these asperities are in a state of plastic creep [Linker and Dieterich, 1992, Baumberger and Caroli, 2006, Dieterich and Kilgore, 1994], the central motivation behind using both the P- and S- phases was that the sensitivity of shear waves to contact-scale deformation under composite loading (normal stresses of a few MPa and a shear loading that drives slip) would be different, and hence complementary, to that of compressional waves.

4.1 Motivation for measuring P- and S-transmissivities simultaneously

To understand the usefulness of simultaneously using the P- and S-transmitted phases, it is instructive to consider some approximate theories of wave propagation across an imperfect interface. We consider a 1-D (imperfect) frictional interface modeled as a periodic, linear array of cracks (top panels in Figure 8) being probed by ultrasonic waves of wavelength 2-3 orders of magnitude longer than the linear dimension of the cracks. In this quasi-static limit (for such long wavelengths, the effect of wave propagation across the array of fractures is well approximated by a static loading), one can disregard any wave scattering due to the presence of cracks and treat the interface as a displacement discontinuity (considering the interface as purely elastic) with its magnitude scaling inversely with an interfacial stiffness (both normal and shear, under the assumption of continuity of stresses across the interface) [Pyrak-Nolte et al., 1990]. Therefore, wave reflectivity and transmis-

sivity across this 'effective interface medium' is a function of the interfacial stiffness; for an incident wave of frequency ω, medium impedance $Z_\alpha = \rho v_\alpha$ and interfacial stiffness κ_α, the transmissivity ($|T_\alpha|$) is given by $|T|_\alpha = 2(\kappa_\alpha/Z_\alpha)/[4(\kappa_\alpha/Z_\alpha)^{1/2} + \omega^2]$ where α denotes different choices between P-, SH- and SV- phases [Pyrak-Nolte et al., 1990].

The interfacial stiffness of an array of cracks can be derived from an analysis of their response to an applied static load. Baik and Thompson [1984] derived relationships between the interfacial stiffness and the ratio of the separations between adjacent tips (W in Figure 8A) and centers (S in Figure 8B) of a 1-D array of co-linear cracks and a 2-D array of co-planar circular asperities. The mode I (P), mode II (SV) and mode III (SH) stiffnesses all obey these relationships to within a multiplicative factor, and hence the corresponding percentage changes in $|T|$ would be identical for these purely elastic models.

However, in the limit $W/S \ll 1$, the contact stresses are expected to be large enough for the contacts to undergo some plastic deformation. This would lead to a further reduction of the wave transmissivities, by an amount that depends upon the ratio W/L, the amplitude and frequency of the probing waves, and the material effective viscosity. Pyrak-Nolte et al. [1990] developed relationships for the transmission of waves across an interface with elastic contacts and a viscous fluid filling the intervening gaps, by treating the interface jointly as a displacement and a velocity discontinuity. In future work we will extend these results to the case where the contacts themselves are viscoelastic. But based on current knowledge we can hypothesize different effective viscosities, and hence different transmissivity changes, for different incoming waves (e.g., lesser effective viscosity and greater transmissivity changes for S-waves polarized in the direction of slip than for P-waves or S-waves polarized perpendicular to slip). Thus the combined use of P- and S-transmissivities should provide new information on the contact rheology of the frictional interfaces in these experiments.

5 Experimental setup and observations

All our experiments were carried out on the biaxial apparatus in the Penn State Rock Mechanics laboratory. The samples (cm-scale, initially bare granite blocks) were set up in a double-direct shear geometry and two PZT shear-wave transducers, housed within steel blocks, were positioned to transmit ultrasonic waves across the sliding interfaces. The normal stress was held constant at 4 MPa for all these experiments.

We carried out large velocity step increases and decreases (1-3 orders of magnitude) and slide-hold-reslides (up to 5000s duration) at different slide/re-slide rates ($V_{s/r} = 3, 30$ and 100 $\mu m s^{-1}$). The mechanical data were collected at 100 samples/second. The interface was probed with ultrasonic shear waves of frequency 0.5 MHz with 1000 shots per second. This allowed a 10-waveform stack corresponding to each mechanical data sample. The ultrasonic data were recorded at 25 MHz. We recorded 8192 samples per transmitted wave allowing us to study both the mode-converted P- and the S-phases on the waveforms (Figure 8B). For each experimental run, we also use the P- and S-wave arrival times to calculate the evolution in P- and S- travel times with respect to a pre-run stack. The travel times are expected to reflect the effects of dilation/compaction of the interface accompanying the imposed changes in slip rate/shear stresses. Therefore, we

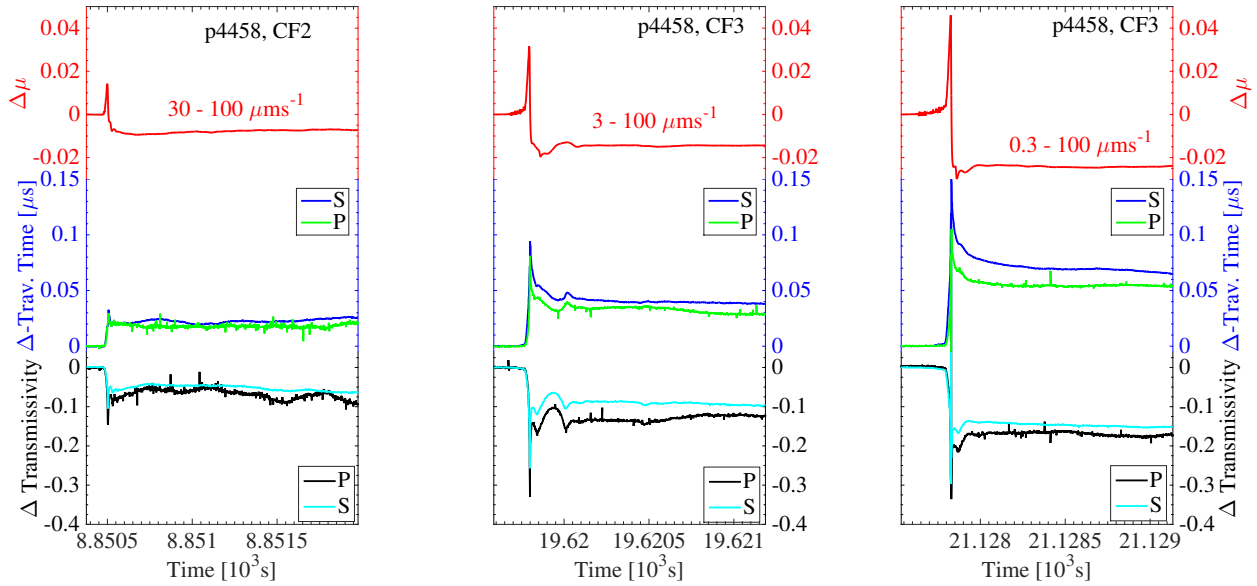

Figure 9: Left to right: Shear stress and ultrasonic responses to 3×, 30×, and 300× velocity step increases plotted versus time (in units of 1000s). The PTA and STA signals show similar characteristic changes and consistent inter-relationships; for example, both PTA and STA decrease rapidly following the velocity step but then recover somewhat in the long-term. The changes in P- and S-travel times are obtained through waveform cross-correlation with a stacked template characterizing the pre- experimental run interface.

have four ultrasonic measurements corresponding to each sample of mechanical data, P- and S-transmitted amplitudes (PTA and STA) and P- and S-differential travel times (ΔTr-time in μs). It is possible that changes in stress in the bulk samples, away from the interface, contribute to changes in transmitted amplitudes and travel times. However, experiments where we propagated waves parallel to the sliding surface suggest that these changes are a small fraction of those for waves propagating perpendicular to the surface. Additional tests of this sort will be conducted to further evaluate this possibility.

Figures 9 and 10 show typical frictional and ultrasonic responses to large velocity step increases and decreases. ΔTransmissivity in these figures is defined as the amplitude A of the transmitted signal at time t minus the amplitude A_{ss} during the prior steady state, normalized by the amplitude of the stacked P- or S-wave template used to define travel time differences. In general both PTA and STA decrease in response to a velocity increase and vice versa. Given the correlations between real contact area fractions (RCA) and PTA/STA arising out of the models of interfaces considered above, we interpret this trend as being due to a smaller RCA at higher sliding rates. The travel times, on the other hand, increase with an increase in the slip rate, presumably due to the shear-induced dilation of the interface.

Nagata et al. [2012] reported an instantaneous decrease (increase) in PTA across a step increase (decrease) in shear stress, and used their observations to argue for a linear shear stress dependence of log state (in addition to the classical slip and time dependence). In our velocity step tests, we also observe that both PTA and STA decrease/increase over the same time scale and vary roughly linearly with the 'step' increases/decreases in shear stress. However, note that the velocity step

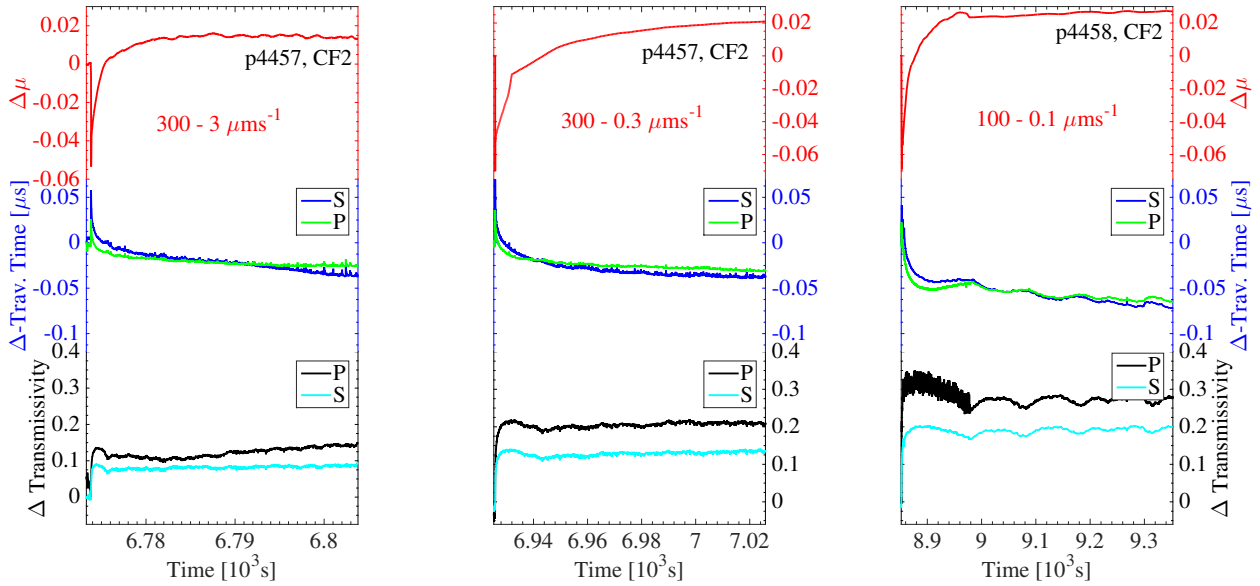

Figure 10: Variations in PTA and STA and P- and S-differential travel time delays across 2 and 3 orders velocity step decreases.

increases in Figure 9 are all either marginally or fully unstable (as evidenced by a rapid drop in stress post peak; also note the remarkable increase in PTA corresponding to the stress drop for the 300× rate step increase) and, hence, the post-peak decrease in shear stress occurs faster and is larger in magnitude than the pre-peak increase. The change in PTA and STA corresponding to this larger and faster shear stress decrease is consistently smaller and slower than for the corresponding increases. This observation does not seem consistent with a systematic linear scaling of PTA/STA with rapid changes in shear stress. In fact it is unclear if PTA/STA is sensitive to shear stress changes or to slip rate changes alone, e.g. the overshoots in PTA/STA in response to the velocity decreases seem more consistent with the expected velocity undershoot following a rapid slip rate decrease.

Figure 11 shows variations in the mechanical and ultrasonic measurements across holds of duration 15s, 300s and 1500s at $V_{s/r} = 30\,\mu m s^{-1}$. The broad features of the ultrasonic data and the inter-relationships between the P- and S-measurements are identical to those observed for the large velocity step decreases in Figure 10. Plotting all the holds at a given $V_{s/r}$ on the same axes, it can be seen that the measurements of STA and PTA are highly reproducible (Figure 12), down to slight deviations of %ΔTransmissivity from linearity with log time (Figure 12E). In terms of percentage changes in transmissivity ($A/A_{ss} - 1$), STA systematically increases more than PTA during these holds (Figures 12A, C and E). This is suggestive of non linearly elastic behavior, and seems consistent with our expectation that contacts subjected to shear waves polarized in the slip direction will exhibit a larger degree of viscous deformation than contacts subjected to normal-incident P waves. However, interpreting these results quantitatively, and making use of the change on P- and S-wave travel times (Figures 12B, D and F), will require extending the analytical results of Pyrak-Nolte et al. [1990] to an interface with elastic and viscous components in series rather than in parallel, and additional experiments in which measurements are made on shear waves polarized

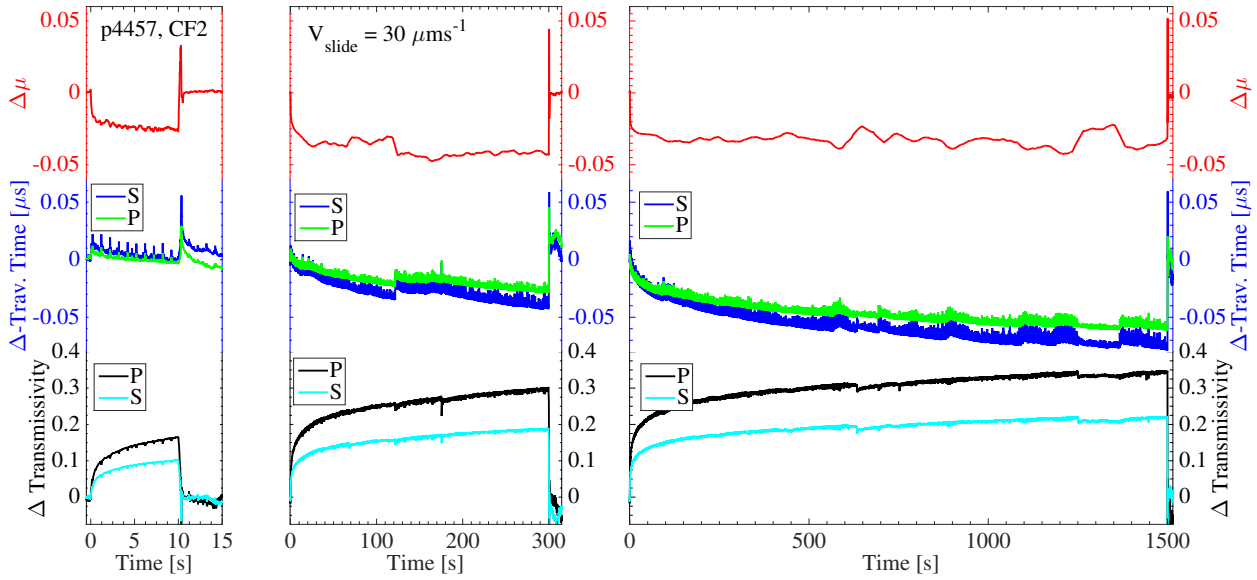

Figure 11: Variations in PTA and STA and P- and S- travel time delays across 15s, 300s and 1500s holds. Note that P- and S- measurement inter-relationships are identical to those seen for large velocity step decreases in Figure 11.

both parallel and perpendicular to the slip direction. This work is currently underway.

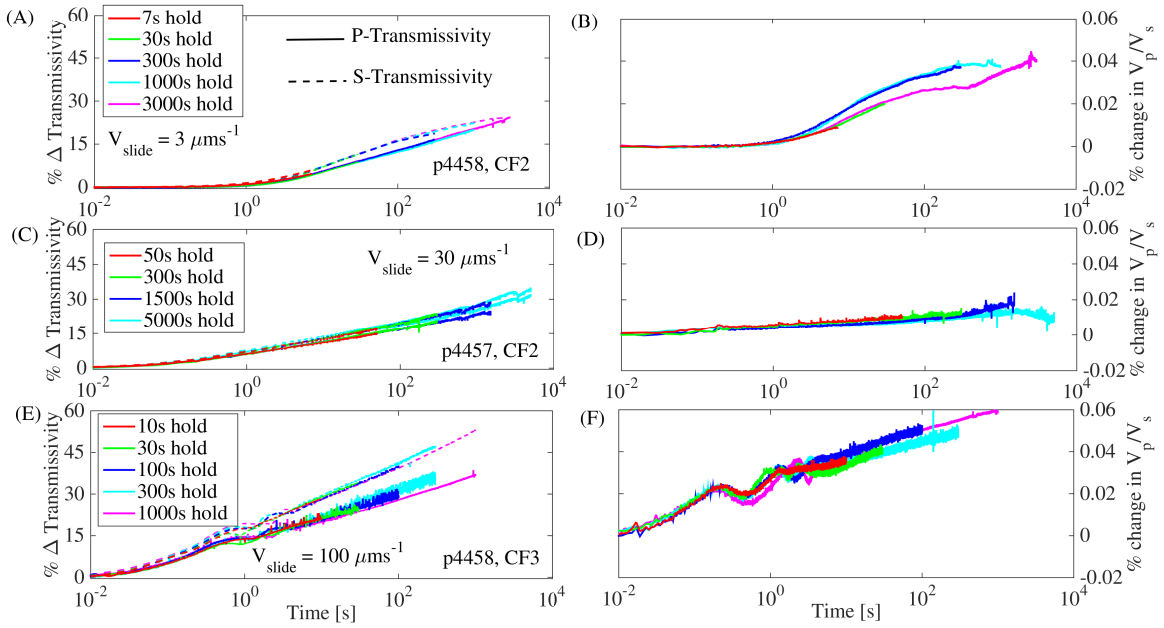

Figure 12: Percent change in PTA and STA and V_p/V_s ratio across all hold sequences in our experiments (A), (B) $V_{\text{slide}} = 3\mu ms^{-1}$; (C), (D) $V_{\text{slide}} = 30\mu ms^{-1}$; and (E), (F) $V_{\text{slide}} = 100\mu ms^{-1}$. Dashed lines on the right panels (Figs. 8A, C, E) depict % change in STA and solid lines show % change in PTA.

References

J. P. Ampuero and A. M. Rubin. Earthquake nucleation on rate and state faults – aging and slip laws. *J. Geophys. Res.*, 113:B01302, 2008.

J-M. Baik and R. B. Thompson. Ultrasonic scattering from imperfect interfaces: A quasi-static model. *J. Nondestruct. Eval.*, 4(3-4):177–196, 1984. ISSN 0195-9298. doi: 10.1007/BF00566223. URL `http://dx.doi.org/10.1007/BF00566223`.

T. Baumberger and C. Caroli. Solid friction from stick-slip down to pinning and aging. *Adv. Phys.*, 55(3-4):279–348, 2006. doi: 10.1080/00018730600732186. URL `http://dx.doi.org/10.1080/00018730600732186`.

N.M. Beeler, T. E. Tullis, and J. D. Weeks. The roles of time and displacement in the evolution effect in rock friction. *Geophys. Res. Lett.*, 21:1987–1990, 1994.

P. Berthoud, T. Baumberger, C. G'Sell, and J.-M. Hiver. Physical analysis of the state- and rate-dependent friction law: Static friction. *Phys. Rev. B*, 59:14313–14327, Jun 1999. doi: 10.1103/PhysRevB.59.14313. URL `http://link.aps.org/doi/10.1103/PhysRevB.59.14313`.

P. Bhattacharya and A. M. Rubin. Frictional response to velocity steps and 1-D fault nucleation under a state evolution law with stressing-rate dependence. *J. Geophys. Res.: Solid Earth*, 119(3):2272–2304, 2014. doi: 10.1002/2013JB010671. URL `http://dx.doi.org/10.1002/2013JB010671`.

P. Bhattacharya, A. M. Rubin, E. Bayart, H. M. Savage, and C. Marone. Critical evaluation of state evolution laws in rate and state friction: Fitting large velocity steps in simulated fault

gouge with time-, slip-, and stress-dependent constitutive laws. *Journal of Geophysical Research: Solid Earth*, 120(9):6365–6385, 2015. ISSN 2169-9356. doi: 10.1002/2015JB012437. URL http://dx.doi.org/10.1002/2015JB012437. 2015JB012437.

P. Bhattacharya, A. M. Rubin, and N. M. Beeler. Does fault strengthening in laboratory rock friction experiments really depend primarily upon time and not slip? *Journal of Geophysical Research: Solid Earth*, 122(8):6389–6430, 2017. ISSN 2169-9356. doi: 10.1002/2017JB013936. URL http://dx.doi.org/10.1002/2017JB013936. 2017JB013936.

M. L. Blanpied, C. J. Marone, D. A. Lockner, J. D. Byerlee, and D. P. King. Quantitative measure of the variation in fault rheology due to fluid-rock interactions. *J. Geophys. Res.*, 103(B5): 9691–9712, 1998.

M. S. Boettcher, G. Hirth, and B. Evans. Olivine friction at the base of oceanic seismogenic zones. *Journal of Geophysical Research: Solid Earth*, 112(B1):n/a–n/a, 2007. ISSN 2156-2202. doi: 10.1029/2006JB004301. URL http://dx.doi.org/10.1029/2006JB004301.

L Bureau, T Baumberger, and C Caroli. Rheological aging and rejuvenation in solid friction contacts. *Eur. Phys. J. E: Soft Matter and Biological Physics*, 8(3):331–337, 2002.

J. H. Dieterich. Time-dependent friction in rocks. *J. Geophys. Res.*, 77(20):3690–3697, 1972.

J. H. Dieterich. Time-dependent friction and the mechanics of stick-slip. *Pure Appl. Geophys.*, 116 (4-5):790–806, 1978.

J. H. Dieterich and B. D. Kilgore. Direct observation of frictional contacts: New insights for state-dependent properties. *Pure Appl. Geophys.*, 143:283–302, 1994.

S. J. Dokos. Sliding friction under extreme pressures. *J. Appl. Mech.*, 13A:148 – 156, 1946.

F. Heslot, T. Baumberger, B. Perrin, B. Caroli, and C. Caroli. Creep, stick-slip, and dry-friction dynamics: Experiments and a heuristic model. *Phys. Rev. E*, 49:4973–4988, Jun 1994. doi: 10.1103/PhysRevE.49.4973. URL http://link.aps.org/doi/10.1103/PhysRevE.49.4973.

S. L. Karner and C. Marone. The effect of shear load on frictional healing in simulated fault gouge. *Geophysical Research Letters*, 25(24):4561–4564, 1998. ISSN 1944-8007. doi: 10.1029/1998GL900182. URL http://dx.doi.org/10.1029/1998GL900182.

S. L. Karner and C. Marone. Frictional restrengthening in simulated fault gouge: Effect of shear load perturbations. *J. Geophys. Res.: Solid Earth*, 106(B9):19319–19337, 2001. ISSN 2156-2202. doi: 10.1029/2001JB000263. URL http://dx.doi.org/10.1029/2001JB000263.

N. Kato and T. E. Tullis. A composite rate- and state-dependent law for rock friction. *Geophys. Res. Lett.*, 28(6):1103–1106, 2001.

B. D. Kilgore, J. Lozos, N. Beeler, and D. Oglesby. Laboratory observations of fault strength in response to changes in normal stress. *J. App. Mech.*, 79(3):31007–1–31007–10, 2012. doi: 10.1115/1.4005883. URL http://dx.doi.org/10.1115/1.4005883.

M. F. Linker and J. H. Dieterich. Effects of variable normal stress on rock friction: Observations and constitutive equations. *J. Geophys. Res.*, 97(B4):4923–4940, 1992.

C. Marone. Laboratory derived fricition laws and their application to seismic faulting. *Annu. Rev. Earth Planet. Sci.*, 26:643–696, 1998.

C. Marone and D. M. Saffer. The mechanics of frictional healing and slip instability during the seismic cycle. In Gerald Schubert, editor, *Treatise on Geophysics*. Elsevier, 2 edition, 2015. to be published.

K. Nagata, M. Nakatani, and S. Yoshida. Monitoring frictional strength with acoustic wave transmission. *Geophys. Res. Lett.*, 35:L06310, 2008.

K. Nagata, M. Nakatani, and S. Yoshida. A revised rate- and state-dependent friction law obtained by constraining constitutive and evolution laws separately with laboratory data. *J. Geophys. Res.*, 117:B02314, 2012.

K. Nagata, B. D. Kilgore, N. Beeler, and M. Nakatani. High-frequency imaging of elastic contrast and contact area with implications for naturally observed changes in fault properties. *J. of Geophys. Res.: Solid Earth*, 119(7):5855–5875, 2014. ISSN 2169-9356. doi: 10.1002/2014JB011014. URL `http://dx.doi.org/10.1002/2014JB011014`. 2014JB011014.

M. Nakatani. Conceptual and physical clarification of rate and state friction: Frictional sliding as a thermally activated rheology. *J. Geophys. Res.*, 106(B7):13,347–13,380, 2001.

M. Nakatani and H. Mochizuki. Effects of shear stress applied to surfaces in stationary contact on rock friction. *Geophys. Res. Lett.*, 23(8):869–872, 1996. ISSN 1944-8007. doi: 10.1029/96GL00726. URL `http://dx.doi.org/10.1029/96GL00726`.

L. J. Pyrak-Nolte, L. R. Myer, and N. G. W. Cook. Anisotropy in seismic velocities and amplitudes from multiple parallel fractures. *J. Geophys. Res.: Solid Earth*, 95(B7):11345–11358, 1990. ISSN 2156-2202. doi: 10.1029/JB095iB07p11345. URL `http://dx.doi.org/10.1029/JB095iB07p11345`.

J. R. Rice. Spatio-temporal complexity of slip on a fault. *J. Geophys. Res.*, 98(B6):9885–9907, 1993.

J. R. Rice, N. Lapusta, and K. Ranjith. Rate and state dependent friction and the stability of sliding between elastically deformable solids. *Journal of the Mechanics and Physics of Solids*, 49(9):1865 – 1898, 2001. ISSN 0022-5096. doi: http://dx.doi.org/10.1016/S0022-5096(01)00042-4. URL `http://www.sciencedirect.com/science/article/pii/S0022509601000424`. The {JW} Hutchinson and {JR} Rice 60th Anniversary Issue.

A. M. Rubin and J. P. Ampuero. Earthquake nucleation on (aging) rate and state faults. *J. Geophys. Res.*, 110:B11312, 2005. doi: 10.1029/2005JB003686.

A. Ruina. *Friction laws and instabilities: a quasistatic analysis of some dry frictional behavior*. PhD thesis, Division of Engineering, Brown University, Providence, Rhode Island, 1980.

A. Ruina. Slip instability and state variable friction laws. *J. Geophys. Res.*, 88:10,359–370, 1983.

T. E. Tullis and J. D. Weeks. Constitutive behavior and stability of frictional sliding of granite. *Pure Appl. Geophys.*, 124(3):383–414, 1986.